Duke Energy®

DAVE BAXTER
Vice President
Oconee Nuclear Station

Duke Energy
ONO1VP / 7800 Rochester Highway
Seneca, SC 29672

864-873-4460
864-873-4208 fax
dabaxter@dukeenergy.com

December 18, 2009

U. S. Nuclear Regulatory Commission
Attn: Document Control Desk
Washington, D. C. 20555-0001

Subject: Duke Energy Carolinas, LLC
Oconee Nuclear Station, Units 1, 2, and 3
Docket Numbers 50-269, 50-270, and 50-287
Request For Additional Information Regarding Proposed License Amendment Request for Methodology Report DPC-NE-1006-P, "Oconee Nuclear Design Methodology Using CASMO-4 / SIMULATE-3"
License Amendment Request No. 2009-02

References:
1. DPC-NE-1004-A, "Nuclear Design Methodology Using CASMO-3/SIMULATE-3P", Rev. 1a, January 2009.
2. DPC-NE-1005-PA, "Nuclear Design Methodology Using CASMO-4/SIMULATE-3 MOX", Rev. 1, November 2008.

On June 10, 2009, Duke Energy Carolinas, LLC (Duke) hereby submitted a license amendment request (LAR) for the Oconee Nuclear Station Renewed Facility Operating License (FOL). Specifically, Duke requested Nuclear Regulatory Commission (NRC) review and approval of methodology report DPC-NE-1006-P, "Oconee Nuclear Design Methodology Using CASMO-4 / SIMULATE-3." Duke currently performs reload design analysis for Oconee Nuclear Station (ONS) using CASMO-3 / SIMULATE-3 (Reference 1). As part of a continuous effort to improve design methods, this methodology report is presented to seek NRC review and approval for the CASMO-4 / SIMULATE-3 nuclear design methodology. Methodology report DPC-NE-1006-P, "Oconee Nuclear Design Methodology Using CASMO-4 / SIMULATE-3," describes the methodology for application to core designs containing low enriched uranium (LEU) fuel bearing lumped burnable and/or gadolinia integral absorbers and its associated technical justification. This methodology is consistent with that used for the McGuire and Catawba Nuclear Stations reload core designs (Reference 2).

On November 2, 2009, Duke received an electronic request for additional information (RAI). The responses are contained in Enclosure 2 (proprietary version) and Enclosure 3 (non-proprietary version).

This response contains information that is proprietary to Duke. In accordance with 10 CFR 2.390, Duke requests that this information be withheld from public disclosure. Enclosure 1 contains the original Affidavit provided with the June 10, 2009, LAR, attesting to the proprietary

Enclosure 2 contains Proprietary Information-Withhold under 10 CFR 2.390.
Upon removal of Enclosure 2, this letter is uncontrolled.

A001
NRR

nature of the information in the methodology report. This Affidavit is applicable to subsequent revisions to the report. The proprietary information is owned by Duke and has substantial commercial value that provides a competitive advantage. Enclosure 2 contains the proprietary version. The non-proprietary version is included in Enclosure 3.

No new commitments are being made as a result of this response. Duke requests approval of the LAR by March 31, 2010.

In accordance with Duke administrative procedures and the Quality Assurance Program Topical Report, these proposed changes to the license are still bounded by the initial review and approval of the Plant Operations Review Committee and Nuclear Safety Review Board. Additionally, a copy of this license amendment request is being sent to the State of South Carolina in accordance with 10 CFR 50.91 requirements.

Inquiries on this proposed amendment request should be directed to Reene' Gambrell of the Oconee Regulatory Compliance Group at (864) 873-3364.

I declare under penalty of perjury that the foregoing is true and correct. Executed on December 18, 2009.

Sincerely,

Dave Baxter, Vice President
Oconee Nuclear Site

Enclosures:

1. Notarized Affidavit of T. C. Geer
2. Requests for Additional Information – Proprietary
3. Requests for Additional Information – Non-Proprietary

bc w/enclosures and attachments:

Mr. Luis Reyes, Regional Administrator
U. S. Nuclear Regulatory Commission - Region II
Atlanta Federal Center
61 Forsyth St., SW, Suite 23T85
Atlanta, Georgia 30303

Mr. John Stang, Project Manager
Office of Nuclear Reactor Regulation
U. S. Nuclear Regulatory Commission
Mail Stop O-8 G9A
Washington, D. C. 20555

Mr. Andy Sabisch
Senior Resident Inspector
Oconee Nuclear Site

Susan E. Jenkins, Manager,
Infectious and Radioactive Waste Management Section
2600 Bull Street
Columbia, SC 29201

ENCLOSURE 1

AFFIDAVIT OF T. C. GEER

AFFIDAVIT OF T. C. GEER

1. I am Vice President of Duke Energy Corporation, and as such have the responsibility of reviewing the proprietary information sought to be withheld from public disclosure in connection with nuclear plant licensing and am authorized to apply for its withholding on behalf of Duke.

2. I am making this affidavit in conformance with the provisions of 10 CFR 2.390 of the regulations of the Nuclear Regulatory Commission (NRC) and in conjunction with Duke's application for withholding which accompanies this affidavit.

3. I have knowledge of the criteria used by Duke in designating information as proprietary or confidential.

4. Pursuant to the provisions of paragraph (b) (4) of 10 CFR 2.390, the following is furnished for consideration by the NRC in determining whether the information sought to be withheld from public disclosure should be withheld.

   (i) The information sought to be withheld from public disclosure is owned by Duke and has been held in confidence by Duke and its consultants.

   (ii) The information is of a type that would customarily be held in confidence by Duke. The information consists of analysis methodology details, analysis results, supporting data, and aspects of development programs, relative to a method of analysis that provides a competitive advantage to Duke.

   (iii) The information was transmitted to the NRC in confidence and under the provisions of 10 CFR 2.390, it is to be received in confidence by the NRC.

   (iv) The information sought to be protected is not available in public to the best of our knowledge and belief.

   (v) The Duke proprietary information sought to be withheld in the submittal is that which is marked in the proprietary version of the Duke methodology report DPC-NE-1006-P, "Oconee Nuclear Design Methodology Using CASMO-4 / SIMULATE-3." This information enables Duke to:

(Continued)

Thomas C. Geer
T. C. Geer

(a) Support license amendment and Technical Specification revision request for its Oconee reactors.

(b) Perform nuclear design calculations on Oconee reactor cores.

(c) Perform transient and accident analysis calculations for Oconee.

(vi) The proprietary information sought to be withheld from public disclosure has substantial commercial value to Duke.

(a) Duke uses this information to reduce vendor and consultant expenses associated with supporting the operation and licensing of nuclear power plants.

(b) Duke can sell the information to nuclear utilities, vendors, and consultants for the purpose of supporting the operation and licensing of nuclear power plants.

(c) The subject information could only be duplicated by competitors at similar expense to that incurred by Duke.

5. Public disclosure of this information is likely to cause harm to Duke because it would allow competitors in the nuclear industry to benefit from the results of a significant development program without requiring a commensurate expense or allowing Duke to recoup a portion of its expenditures or benefit from the sale of the information.

(Continued)

T. C. Geer

Thomas C. Geer affirms that he is the person who subscribed his name to the foregoing statement, and that all the matters and facts set forth herein are true and correct to the best of his knowledge.

Thomas C. Geer

T. C. Geer

Subscribed and sworn to me: June 8, 2009
Date

Freda K. Crump

Notary Public

My Commission Expires: August 17, 2011

SEAL

FREDA K CRUMP
NOTARY
PUBLIC
LINCOLN COUNTY, NC

ENCLOSURE 3

REQUEST FOR ADDITIONAL INFORMATION

DPC-NE-1006-P

Oconee Nuclear Design Methodology Using CASMO-4 / SIMULATE-3

NON-PROPRIETARY VERSION

REQUEST FOR ADDITIONAL INFORMATION
DPC-NE-1006-P, OCONEE NUCLEAR DESIGN METHODOLOGY USING CASMO-4 / SIMULATE-3

REQUEST FOR ADDITIONAL INFORMATION (RAI) 1:

Duke Energy (Duke) staff revisits the list of RAIs for the DPC-NE-1005-P, Revision 1, and consider the applicability of each of the RAI to DPC-NE-1006-P. In each of the RAIs for DPC-NE-1005-P, address the applicability to DPC-NE-1006-P.

If any of the RAI question(s) requested in the review of DPC-NE-1005-P, Revision 1, is not applicable to DPC-NE-1006-P, please state why so and provide a qualitative technical basis in support of your position.

RAI #1 RESPONSE:

During the review of DPC-NE-1006-P, titled "Oconee Nuclear Design Methodology Using CASMO-4/SIMULATE-3", the NRC issued four questions in a RAI related to the use of the CASMO-4/SIMULATE-3 computer codes and the nuclear design methodology. To expedite the review process of DPC-NE-1006-P the NRC staff took advantage of the RAIs generated in the course of the review of DPC-NE-1005-PA, Revision 1, titled "Nuclear Design Methodology Using CASMO-4/SIMULATE-3 MOX" (applicable to McGuire and Catawba Nuclear Stations), and re-issued the 19 questions for methodology report DPC-NE-1006-P as question 1. Not all of the RAIs for DPC-NE-1005-PA, Revision 1, will be pertinent to DPC-NE-1006-P. As such, the NRC staff has requested that Duke revisit the list of RAIs for DPC-NE-1005-PA, Revision 1, and consider their applicability to DPC-NE-1006-P. If any of the RAIs are not applicable to DPC-NE-1006-P, the NRC staff has requested Duke to provide a qualitative technical basis in support of the position.

NOTE: Questions 1 - 19 (denoted Q1 – Q19) are the re-issued questions from the review of DPC-NE-1005-PA, Revision 1. References to sections/paragraphs, pages, tables, figures or references, as such, in these questions are from DPC-NE-1005-PA, Revision 1. If applicable to Oconee, responses will include the corresponding sections/paragraphs, pages, tables, figures or references from DPC-NE-1006-P.

In the process of developing DPC-NE-1006-P an effort was made to address the NRC RAIs received during the review of DPC-NE-1005-PA, Revision 1. As such some responses will reference specific sections/paragraphs, pages, tables, figures or references of DPC-NE-1006-P and not provide additional clarification details.

Q1: Page B1-1, paragraph 2 indicates that the CASMO-4/SIMULATE-3 code system has been previously used to model fuel designs with gadolinia. Please provide a qualitative and quantitative assessment of how the uncertainty results in this report compare to the results of those previous applications.

Q1 RESPONSE:

Four references were cited in the third paragraph of Chapter 1 that provided previously performed benchmark results that compared the CASMO-4/SIMULATE-3 analytical models against measured gadolinia data. The references cited were:

1. DPC-NE-1005-PA, Revision 1, "Nuclear Design Methodology Using CASMO-4/SIMULATE-3 MOX", November 2008.

2. "Gadolinia Depletion Analysis by CASMO-4", Y. Kobayashi, E. Saji (Toden Software - Japan), A. Toba (TEPCO-Japan), November 1993.
3. "CASMO-4/SIMULATE-3 Benchmarking Against VIP-PWR MOX Fuel Critical Experiment", M. Mori, M. Kawamura, S. Inoue, April 1994.
4. "Prairie Island Nuclear Power Plant Qualification of Reactor Physics Methods for Application to Prairie Island", NSPNAD-8101-A, Revision 2, October 2000.

The conclusions reached in each of the benchmark calculations were that the CASMO-4/SIMULATE-3 code system is capable of accurately reproducing measured results (isotopic, reactivity or power distribution) for fuel containing gadolinia, consistent with Duke's benchmark results.

Reference 2 describes the benchmark of the CASMO-4 micro region depletion model against measured data from depleted gadolinia (Gd_2O_3) bearing fuel pins (GAD pins). The measured data were generated from irradiation experiments performed with high GAD pin concentration of 6 and 9 w/o Gd_2O_3 conducted at the Halden reactor in Norway. CASMO-4 benchmark calculations were performed against the following measured data from the Halden experiments:

- Pellet-average atom fractions of gadolinium (Gd) isotopes as a function of exposure
- Radial distribution of Gd isotopes at several exposures

Good agreement between measured and calculated pellet-average atom fractions for the Gd^{155} and Gd^{157} isotopes as a function of pin exposure was observed for both the 6 and 9 w/o GAD pins. Comparison of the CASMO-4 calculated and measured radial distribution of the Gd^{155} and Gd^{157} isotopes also showed good agreement between calculated and measured results. The conclusion of the benchmark calculation was that CASMO-4 can predict both the spatial behavior of Gd depletion within a fuel pin and the average number densities of the most important Gd isotopes for GAD pins with high concentrations of Gd with a high degree of accuracy. The high concentration of Gd modeled in these experiments is consistent with the range of GAD pin concentrations included in the Three Mile Island (TMI) benchmark results and is representative of the concentrations required for current generation core designs.

Figure 3-7 of the TMI gadolinia fuel cycle benchmark calculation shows the difference between measured and predicted hot full power (HFP) ARO critical boron concentrations as a function of burnup. The good agreement between measured and predicted core reactivity as a function of burnup shown in Figure 3-7 independently confirms the accuracy of the micro-depletion model in CASMO-4. The results shown in Figure 3-8 compare the TMI gadolinia fuel cycles measured minus predicted boron deviations with the same data from the Oconee fuel cycle designs with boron-based lumped burnable poison rod (i.e. LBP). The data in Figure 3-8 and in Tables 3-6 and 3-13 indicate that the CASMO-4/SIMULATE-3 analytical models are at least as good at predicting core reactivity for fuel cycles containing gadolinia integral absorbers relative to those with conventional boron-based lumped burnable absorbers. The excellent behavior of the calculated core reactivity with burnup as shown by the measured minus predicted boron deviations as a function of burnup in Figures 3-7 and 3-8 independently validates the conclusion reached in Reference 2 that the CASMO-4 micro depletion model can accurately predict the depletion of high concentration gadolinia fuel. The average measured minus predicted deviation in the CASMO-4/SIMULATE-3 model from the TMI gadolinia benchmark calculations, as shown in Table 3-13, was 15 ppmB with a standard deviation of 17 ppmB.

Reference 3 describes the benchmark of the CASMO-4/SIMULATE-3 code systems' analytical models for calculating pin power distributions for mixed oxide (MOX) fuel and gadolinia (Gd_2O_3)

bearing UO_2 fuel (GAD). The benchmark calculations consisted of comparing both CASMO-4 and SIMULATE-3 calculated pin powers against measured pin powers for both MOX and GAD fuel pins. The measured results were obtained from the VENUS International Program (VIP) critical experiments performed at the VENUS critical facility in Belgium. The results from these critical experiments are relevant to boron-based and gadolinia-based core designs because they demonstrate the accuracy and robustness of the CASMO-4/SIMULATE-3 analytical models for accurately modeling steep thermal flux gradients. These gradients are representative of gradients between UO_2 fuel (LEU) pins and lumped burnable poison pins or gadolinia fuel (GAD) pins.

The benchmark calculation presented in Reference 3 included a MOX fuel assembly surrounded by all LEU fuel, and a MOX fuel assembly with 20 GAD fuel pins surrounded by all LEU fuel. The MOX fuel consisted of 14.4 w/o Pu^{tot}, 9.7 w/o Pu^{tot} and 5.4 w/o Pu^{tot} MOX fuel pins. The 20 GAD pins consisted of 7.18 w/o Gd_2O_3 and 3.47 w/o U-235. The pin power distribution was inferred from fission rate measurements performed by gamma scanning.

Comparisons between both CASMO-4 and SIMULATE-3 predicted and measured pin powers for both MOX and GAD pins were performed in Reference 3. Excellent agreement between predicted and measured pin powers was observed for both the CASMO-4 and SIMULATE-3 codes. The root mean square (RMS) error for CASMO-4 and SIMULATE-3 predicted pin powers for core locations with gadolinia were 2.1% and 1.1% respectively from information presented in Figures 5 and 10 (Reference 3) based on equal weighting of each core location. This compares to the CASMO-4 and SIMULATE-3 RMS errors for GAD pin locations from the evaluation of the B&W critical experiments, also based on equal weighting of each core location, of [ ] respectively. This is good agreement given the small sample size and low power density of the GAD pins. In summary, Reference 3 showed that both CASMO-4 and SIMULATE-3 were capable of accurately calculating pin power distributions for complicated core geometries consisting of LEU, MOX and GAD fuel pins. The results presented in the B&W critical benchmark calculation showed similar performance for fuel lattices containing LEU and GAD fuel pins.

Reference 4 describes the benchmark of the CASMO-4/SIMULATE-3 code system to measurements performed at the Northern States Power (NSP) Company's Prairie Island (PI) Nuclear Generating Plant. PI is a two loop pressurized water reactor containing 121 14x14 fuel assemblies. CASMO-4/SIMULATE-3 benchmark calculations were performed against six cycles of PI measured data that contained gadolinia bearing fuel up to 8.0 w/o Gd_2O_3. The results showed that the CASMO-4/SIMULATE-3 code system produced power distribution reliability factors that were less than those generated from previously licensed methods. The benchmark results also showed that the CASMO-4/SIMULATE-3 code system could accurately predict core reactivity (see Table 1).

Reference 1 describes the benchmark, performed by Duke, of the CASMO-4/SIMULATE-3 code system to measurements performed at the Tennessee Valley Authority's (TVA) Sequoyah Nuclear Generating Plant (Unit-2). This plant is a four loop pressurized water reactor containing 193 17x17 fuel assemblies. CASMO-4/SIMULATE-3 benchmark calculations were performed against five cycles of measured data that contained gadolinia bearing fuel up to 8.0 w/o Gd_2O_3. The benchmark results showed that the CASMO-4 / SIMULATE-3 code system could accurately predict core reactivity (see Table 1). The results also showed that the CASMO-4/SIMULATE-3 code system produced power distribution reliability factors that were consistent with those generated from previously licensed methods (see Table 2).

Table 1 compares benchmark results from PI (performed by NSP), Sequoyah (performed by Duke) and TMI (performed by Duke – documented in DPC-NE-1006-P) of the HFP and beginning of cycle (BOC) HZP soluble boron concentrations, BOC HZP control rod worths and BOC HZP isothermal temperature coefficients for reactor cores containing gadolinia. PI data was not available to perform HFP ARO soluble boron concentration comparisons. The PI statistical results were calculated from data contained in Tables 3.1.1, 3.2.1 and 4.3.1 from Reference 4. The Sequoyah data was taken from Table B3-11 of Reference 1. All differences are defined as measured minus predicted. All relative differences are defined as measured minus predicted values divided by predicted values. The CASMO-4/SIMULATE-3 benchmark results shown in Table 1 indicate that Duke HFP and BOC HZP soluble boron concentrations, BOC HZP control rod worths and BOC HZP isothermal temperature coefficients are predicted with comparable accuracy relative to measured values.

Table 1
Summary Comparison of Core Reactivity Benchmark Results

Parameter	Plant	Mean	Std Dev.
BOC HZP Soluble Boron Concentration (ppmB)	PI (NSP) (Reference 4)	11	10
BOC HZP Control Rod Worth (%)		0.8	4.2
BOC HZP Isothermal Temperature Coefficient (pcm/°F)		-1.0	0.53
BOC HZP Soluble Boron Concentration (ppmB)	Sequoyah (Duke) (Reference 1)	-12	10
HFP Critical Soluble Boron (ppmB)		-11	11
BOC HZP Control Rod Worth (%)		-2.7	3.5
BOC HZP Isothermal Temperature Coefficient (pcm/°F)		-1.0	0.14
BOC HZP Soluble Boron Concentration (ppmB)	TMI (Duke) (Reference DPC-NE-1006-P)	5.5	37.3
HFP Critical Soluble Boron (ppmB)		14.9	17.4
BOC HZP Control Rod Worth (%)		-3.7	2.8
BOC HZP Isothermal Temperature Coefficient (pcm/°F)		-0.8	0.2

Table 2 compares benchmark results from Sequoyah (performed by Duke in Reference 1) and TMI (performed by Duke – documented in DPC-NE-1006-P) of the power distribution reliability factors for reactor cores containing gadolinia. The Sequoyah data was taken from Table B3-10 of Reference 1. Power distribution reliability factors between Duke and NSP cannot be directly compared because of differences in statistical methods and assumptions used to derive radial and total power distribution uncertainty factors. As Duke understands them, some of the more important differences include:

a. The NSP methodology only compares predicted and measured reaction rates for instrumented core locations. The Duke methodology compares predicted and measured powers for instrumented and non-instrumented core locations with measured relative powers greater than 1.0.
b. The NSP methodology calculates 95/95 FΔH and Fq uncertainty factors based on the difference between predicted and measured reaction rates. The Duke methodology

calculates FΔH and Fq uncertainty factors based on relative differences between predicted and measured powers.

c. The NSP methodology does not calculate an Fz uncertainty.

Table 2
Power Distribution Reliability Factors Comparison

Parameter	Analysis	Bias	Statistical Deviation ($K_a\sigma_a$)	Assembly Uncertainty Factor (ONRF)
FΔH	Sequoyah (Duke) (Reference 1)	[ ]	[ ]	[ ]
Fq		[ ]	[ ]	[ ]
Fz		[ ]	[ ]	[ ]
FΔH	TMI (Duke) (Reference DPC-NE-1006-P)	0.00224	0.02904	1.0268
Fq		-0.00158	0.03532	1.0369
Fz		-0.00475	0.02035	1.0251

The gadolinia-based reactor core reactivity and power distribution benchmark results summarized in Tables 1 and 2, respectively are consistent with the boron-based reactor core benchmark results summarized in Tables 3-6 and 3-5, respectively of DPC-NE-1006-P.

In summary, the CASMO-4/SIMULATE-3 code system has been thoroughly benchmarked against reactor cores containing high numbers and concentrations of both boron-based and gadolinia-based burnable absorbers. These core designs result in local steep thermal flux gradients between UO_2 fuel pins, and boron-based and gadolinia-based burnable absorber pins. The results presented in DPC-NE-1006-P indicated comparable accuracy for the CASMO-4/SIMULATE-3 code system applied to Oconee relative to Duke's previously approved methodology. As a result, the qualitative expectation is that since previous benchmarks have shown that the CASMO-4 / SIMULATE-3 code system is capable of accurately modeling reactor cores with boron-based (lumped) and gadolinia-based (integral) burnable absorber pins, the CASMO-4/SIMULATE-3 analytical models should be equally capable of modeling Oconee reactor cores with gadolinia with similar accuracy. This expectation was confirmed by the TMI benchmark calculations presented in DPC-NE-1006-P which extensively benchmarked the CASMO-4/SIMULATE-3 code system against both transition and equilibrium fuel cycles containing both low and high concentrations of gadolinia.

Q2: a) Page B1-2, paragraph 2 states that due to the diverse core designs used in the Sequoyah benchmarking, the results are considered applicable to future McGuire and Catawba core designs. Please provide details on the gadolinia concentrations and fuel assembly designs planned for upcoming McGuire and Catawba core designs.

b) If available, please provide the calculated results for the upcoming McGuire and Catawba core designs. Please include calculations of assembly average power distributions, LEU and gadolinia pin power distributions, power distribution peaking factors, and the statistical variance of the power distribution results. The predicted power for the gadolinia pins should be calculated after the gadolinia is depleted, as this is when the gadolinia pin power may become limiting.

Q2a RESPONSE:

The benchmark analysis is performed using TMI data since the plant is similar to Oconee as described in Sections 3.2.1 and 3.1.1 of DPC-NE-1006-P, respectively. The TMI benchmark cores used gadolinia loadings (refer to DPC-NE-1006-P, Table 3-7) that encompass the range of loadings expected to be used for the Oconee core designs.

The fuel assembly design recently implemented at Oconee is the AREVA NP Mark-B-HTP (HTP) fuel assembly design which consists of a 15x15 array of 208 fuel pins, 16 control rod guide tubes and one instrument tube (for additional details refer to DPC-NE-2015-PA, "Oconee Nuclear Station Mark-B-HTP Fuel Transition Methodology). Core reactivity and peaking control is planned to be achieved by the use of soluble boron, lumped boron-based burnable poison rods (LBP) in the guide tubes and gadolinia (Gd_2O_3) integral fuel burnable absorbers. The gadolinia fuel assembly designs currently considered for Oconee consist of fuel pins containing gadolinia concentrations ranging from 2 to 8 w/o Gd_2O_3 and from 4 to 20 gadolinia pins per assembly. To reduce intra-assembly peaking factors, multiple gadolinia enrichments within a fuel lattice may be used. The fuel assemblies containing gadolinia may also contain lumped burnable poison rods as needed to develop acceptable core designs that meet cycle energy and peaking requirements. The number and enrichment of the gadolinia pins may change as experience is gained in designing reactor cores with gadolinia.

RESPONSE to Q2b:

Fuel cycle conceptual designs, analyzed using CASMO-4/SIMULATE-3, utilizing the HTP fuel product with LBP and/or only gadolinia integral fuel burnable absorbers have been performed. The Oconee 2 Cycle 29 (O2C29) core is one such design which utilizes only gadolinia integral fuel burnable absorbers. The O2C29 core design is a 24 month low-leakage fuel cycle design. Results from analysis of this core design were used to generate the requested data. Figure 1 presents the core loading pattern for the O2C29 core. The previous cycle core location of each reinsert fuel assembly, fuel batch identifier, fuel enrichment and burnable absorber loadings for each core location are provided. The core design was depleted at HFP conditions to a burnup of 670 effective full power days (EFPD). Responses to this question were developed from SIMULATE-3 power distribution information calculated from this depletion.

Figures 2 through 5 present the SIMULATE-3 calculated core radial power distributions and limiting pin power details for burnups of 4, 200, 400 and 670 EFPD. Assembly average powers, peak integrated pin powers (FΔH) and the peak pin powers (Fq) are presented. Figures 6 and 7 show core peak integrated pin powers and peak pin powers at nominal HFP conditions as a function of burnup for both UO_2 (LEU) and UO_2+Gd_2O_3 (GAD) fuel pins. As indicated by the data, the GAD fuel pins never exceed the LEU power density.

LEU and GAD fuel pin power distributions for core locations K-12 and K-14 are presented at burnups of 4, 200, 400 and 670 EFPD in Figures 8 through 15. Sample pin power distributions for core location K-12 are presented in Figures 8 through 11 and were chosen because this core location exhibited the highest integated power density (F□H) of feed fuel locations early in cycle. Sample pin power distributions for core location K-14 are presented in Figures 12 through 15 and were chosen for presentation because this core location exhibited the highest Fq of feed fuel locations early in cycle.

The mean and variance of the SIMULATE-3 predicted assembly average powers and peak pin power peaking factors against measured values is not determined since O2C29 is a conceptual core design. The statistical assembly power distribution information is detailed in Chapter 3 of DPC-NE-1006-P.

Figure 1
O2C29 Conceptual Core Loading Pattern

	8	9	10	11	12	13	14	15
H	25N-12 26B 3.53 No BP	FEED 31A 4.50 20N84	28N-09 30A 4.12 16M84	FEED 31A 4.50 20N84	28L-11 30A 4.12 20N84	28H-09 30A 4.12 20N84	FEED 31B 4.81 12K4	28H-14 30B 4.51 12K7
K	FEED 31A 4.50 20N84	28K-12 30A 4.12 16M84	FEED 31A 4.50 20N84	28K-14 30B 4.51 12J4	FEED 31A 4.50 20N84	28M-13 30B 4.51 16M84	FEED 31B 4.81 16M84	28K-10 30A 4.12 20N84
L	28N-09 30A 4.12 16M84	FEED 31A 4.50 20N84	28L-13 30B 4.51 16M84	FEED 31A 4.50 20N84	28N-13 30B 4.51 4A2	FEED 31A 4.50 20N84	FEED 31B 4.81 8E3	28M-14 29A 4.63 300P-8H4
M	FEED 31A 4.50 20N84	28P-09 30B 4.51 12J4	FEED 31A 4.50 20N84	28M-10 30A 4.12 20N84	28L-14 30B 4.51 12J4	FEED 31B 4.81 16M84	28K-15 29A 4.63 250P-8H4	
N	28L-11 30A 4.12 20N84	FEED 31A 4.50 20N84	28O-12 30B 4.51 4A2	28P-10 30B 4.51 12J4	28O-10 30B 4.51 16M84	FEED 31B 4.81 12J5	26L-15 26A 3.33 230P	
O	28H-09 30A 4.12 20N84	28O-11 30B 4.51 16M84	FEED 31A 4.50 20N84	FEED 31B 4.81 16M84	FEED 31B 4.81 12J5	28H-11 30A 4.12 20N84		
P	FEED 31B 4.81 12K4	FEED 31B 4.81 16M84	FEED 31B 4.81 8E3	28R-09 29A 4.63 250P-8H4	26R-10 26A 3.33 230P			
R	28H-14 30B 4.51 12K7	28L-09 30A 4.12 20N84	28P-11 29A 4.63 300P-8H4					

<u>KEY</u>
Previous Cycle Core Location or FEED (fresh fuel)
Fuel Batch ID
Initial Fuel Enrichment (w/o U-235)
Burnable Poison or Burnable Poison History (non-FEED locations)
e.g. 1. 20N84 =20 GAD pins with 4 and 8 w/o Gd_2O_3 (Pattern N)
2. 12J5 = 12 GAD pins with 5 w/o Gd_2O_3 (Pattern J)
3. 300P = 3.00 w/o LBP pulled (history effect)
4. No BP = No LBP and No GAD

Figure 2
O2C29 Conceptual Core Design - Core Radial Power Distribution
HFP, 4 EFPD, Equilibrium Xenon and Samarium

	08	09	10	11	12	13	14	15
H	.7654 .8586 .7903 E-03	1.0951 1.4150 1.2696 M-09	1.0406 1.2367 1.1176 L-11	1.2741 1.6408 1.4549 I-08	1.0862 1.3034 1.1567 A-15	1.0957 1.3538 1.1792 L-11	1.2925 1.7569 1.4972 E-10	.5822 1.0473 .9099 A-15
K	1.0951 1.4150 1.2696 G-13	.9896 1.1870 1.0806 O-15	1.2350 1.6007 1.4300 M-09	1.2123 1.4781 1.3092 K-12	1.3279 1.7704 1.5305 I-13	1.2007 1.5047 1.3150 E-12	1.2123 1.7722 1.5095 A-15	.4939 .9586 .8379 A-01
L	1.0406 1.2367 1.1176 E-12	1.2328 1.5973 1.4272 I-13	1.1418 1.3349 1.2103 L-05	1.3126 1.7188 1.5032 H-07	1.2500 1.6404 1.3821 O-01	1.3042 1.7628 1.5086 C-07	1.1573 1.7632 1.5023 A-01	.3382 .7508 .6582 A-01
M	1.2741 1.6408 1.4549 H-09	1.2108 1.4773 1.3079 L-11	1.3120 1.7183 1.5023 G-08	1.0861 1.2984 1.1553 D-05	1.1467 1.4608 1.2781 E-04	1.1569 1.7369 1.4862 A-01	.5456 1.0541 .9263 A-01	
N	1.0862 1.3034 1.1567 A-01	1.3267 1.7695 1.5295 M-09	1.2503 1.6405 1.3815 A-15	1.1464 1.4613 1.2788 D-05	.9475 1.2030 1.0672 A-01	.8897 1.4667 1.2607 A-01	.2516 .5692 .5062 A-01	
O	1.0957 1.3538 1.1792 E-12	1.1991 1.5041 1.3142 L-05	1.3031 1.7617 1.5077 G-03	1.1554 1.7356 1.4854 A-01	.8884 1.4645 1.2583 A-01	.3793 .8351 .7355 A-01		
P	1.2925 1.7569 1.4972 F-05	1.2092 1.7694 1.5073 O-01	1.1553 1.7606 1.5001 A-01	.5447 1.0521 .9246 A-01	.2513 .5685 .5055 A-01			
R	.5822 1.0473 .9099 A-01	.4904 .9496 .8303 A-01	.3373 .7487 .6565 A-01	Assembly Average Power Assembly Max Fq Maximum 2-D Pin Power Maximum 2-D Pin Power Location				

The maximum assembly power is 1.3279 in assembly K-12.

The maximum Fq factor from 3PINP is 1.7722 in assembly K-14.

The maximum 2-D pin power is 1.5305 in assembly K-12 for pin I-13.

Figure 3
O2C29 Conceptual Core Design - Core Radial Power Distribution
HFP, 200 EFPD, Equilibrium Xenon and Samarium

	08	09	10	11	12	13	14	15
	.8878	1.2816	1.1051	1.3868	1.0574	1.0152	1.2715	.5633
H	1.0443	1.6692	1.3517	1.7876	1.3407	1.2617	1.7592	1.0212
	.9140	1.4187	1.1677	1.5102	1.1528	1.0792	1.4559	.8689
	E-03	M-11	L-11	E-13	A-15	L-11	D-11	A-15
	1.2816	1.0746	1.3785	1.2162	1.3757	1.1306	1.2040	.4838
K	1.6692	1.3256	1.7977	1.4964	1.8280	1.4719	1.7458	.9390
	1.4187	1.1450	1.5220	1.2877	1.5293	1.2514	1.4525	.8016
	E-13	L-11	M-11	K-12	E-13	A-15	A-15	A-01
	1.1051	1.3765	1.1604	1.3676	1.1778	1.3358	1.1514	.3369
L	1.3517	1.7943	1.4081	1.8122	1.5705	1.8013	1.7928	.7524
	1.1677	1.5191	1.2209	1.5245	1.3218	1.4967	1.4818	.6422
	E-12	K-13	K-04	K-03	O-01	C-05	C-05	A-01
	1.3868	1.2149	1.3670	1.0037	1.0286	1.1392	.5372	
M	1.7876	1.4953	1.8110	1.2836	1.3640	1.6768	1.0550	
	1.5102	1.2867	1.5235	1.1149	1.1738	1.4062	.9012	
	C-05	L-11	C-11	A-01	A-01	A-01	A-01	
	1.0574	1.3746	1.1780	1.0284	.8429	.8474	.2516	
N	1.3407	1.8270	1.5705	1.3648	1.0655	1.3738	.5767	
	1.1528	1.5284	1.3214	1.1745	.9320	1.1623	.4991	
	A-01	M-05	A-15	A-01	A-01	A-01	A-01	
	1.0152	1.1295	1.3347	1.1379	.8464	.3590		
O	1.2617	1.4715	1.8003	1.6761	1.3720	.7718		
	1.0792	1.2510	1.4958	1.4055	1.1605	.6682		
	E-12	O-01	E-03	A-01	A-01	A-01		
	1.2715	1.2012	1.1499	.5365	.2513			
P	1.7592	1.7437	1.7907	1.0533	.5761			
	1.4559	1.4509	1.4801	.8999	.4986			
	E-04	O-01	E-03	A-01	A-01			
	.5633	.4808	.3363	Assembly Average Power				
R	1.0212	.9330	.7507	Assembly Max Fq				
	.8689	.7964	.6409	Maximum 2-D Pin Power				
	A-01	A-01	A-01	Maximum 2-D Pin Power Location				

The maximum assembly power is 1.3868 in assembly H-11.

The maximum Fq factor from 3PINP is 1.8280 in assembly K-12.

The maximum 2-D pin power is 1.5293 in assembly K-12 for pin E-13.

Figure 4
O2C29 Conceptual Core Design - Core Radial Power Distribution
HFP, 400 EFPD, Equilibrium Xenon and Samarium

	08	09	10	11	12	13	14	15
	.9508	1.3742	1.1008	1.3935	1.0122	.9596	1.2343	.5658
H	1.0647	1.6758	1.2578	1.6974	1.2282	1.1173	1.5561	.9454
	.9761	1.4956	1.1455	1.5163	1.1087	1.0143	1.3925	.8555
	E-03	L-11	K-12	D-11	A-15	M-11	E-12	A-15
	1.3742	1.0915	1.4099	1.1693	1.3592	1.0743	1.2007	.4921
K	1.6758	1.2525	1.7135	1.3470	1.6918	1.3019	1.5818	.8789
	1.4956	1.1417	1.5305	1.2315	1.5015	1.1881	1.3986	.7926
	E-12	L-11	L-11	E-13	D-11	A-15	D-11	A-01
	1.1008	1.4086	1.1291	1.3627	1.1252	1.3434	1.1256	.3483
L	1.2578	1.7112	1.2970	1.6902	1.3936	1.6797	1.5894	.7179
	1.1455	1.5287	1.1792	1.5093	1.2543	1.4814	1.4097	.6456
	D-11	K-12	K-04	E-04	O-01	D-05	C-05	A-01
	1.3935	1.1686	1.3625	.9667	.9983	1.1909	.5616	
M	1.6974	1.3463	1.6888	1.1910	1.2228	1.6062	.9925	
	1.5163	1.2305	1.5081	1.0800	1.1193	1.4184	.9075	
	E-04	M-05	D-05	A-01	A-01	E-03	A-01	
	1.0122	1.3587	1.1258	.9983	.8518	.9244	.2844	
N	1.2282	1.6917	1.3943	1.2235	1.0256	1.3459	.6041	
	1.1087	1.5011	1.2545	1.1201	.9299	1.1899	.5482	
	A-01	K-04	A-15	A-01	O-01	E-03	A-01	
	.9596	1.0739	1.3432	1.1903	.9237	.4014		
O	1.1173	1.3025	1.6798	1.6060	1.3443	.7911		
	1.0143	1.1883	1.4814	1.4181	1.1886	.7145		
	E-13	O-01	E-04	C-05	C-05	A-01		
	1.2343	1.1990	1.1251	.5613	.2843			
P	1.5561	1.5805	1.5890	.9918	.6039			
	1.3925	1.3976	1.4093	.9069	.5479			
	D-05	K-03	E-03	A-01	A-01			
	.5658	.4898	.3479	Assembly Average Power				
R	.9454	.8749	.7169	Assembly Max Fq				
	.8555	.7890	.6448	Maximum 2-D Pin Power				
	A-01	A-01	A-01	Maximum 2-D Pin Power Location				

The maximum assembly power is 1.4099 in assembly K-10.

The maximum Fq factor from 3PINP is 1.7135 in assembly K-10.

The maximum 2-D pin power is 1.5305 in assembly K-10 for pin L-11.

Figure 5
O2C29 Conceptual Core Design - Core Radial Power Distribution
HFP, 670 EFPD, Equilibrium Xenon and Samarium

	08	09	10	11	12	13	14	15
	.9084	1.2547	1.0098	1.2673	.9695	.9522	1.2138	.6225
H	1.0188	1.4671	1.1488	1.4879	1.1370	1.1014	1.4624	.9786
	.9305	1.3484	1.0448	1.3590	1.0368	1.0026	1.3402	.8937
	E-03	L-11	K-13	E-12	A-15	M-11	E-12	A-15
	1.2547	1.0042	1.2709	1.0819	1.2827	1.0526	1.2124	.5508
K	1.4671	1.1431	1.4934	1.2490	1.5343	1.2552	1.5042	.9128
	1.3484	1.0420	1.3663	1.1391	1.3975	1.1480	1.3769	.8345
	E-12	M-11	L-11	O-15	E-12	A-15	D-11	A-01
	1.0098	1.2703	1.0461	1.2840	1.1538	1.3189	1.1320	.4029
L	1.1488	1.4926	1.1984	1.5249	1.4306	1.5629	1.4861	.7640
	1.0448	1.3657	1.0832	1.3909	1.2587	1.4294	1.3618	.6957
	C-11	K-12	M-05	L-05	L-05	E-12	D-05	A-01
	1.2673	1.0816	1.2841	.9729	1.0398	1.2642	.6363	
M	1.4879	1.2489	1.5251	1.1312	1.2272	1.5686	1.0276	
	1.3590	1.1393	1.3911	1.0337	1.1188	1.4387	.9477	
	D-05	O-15	E-12	A-01	O-01	E-04	A-01	
	.9695	1.2828	1.1546	1.0399	.9406	1.0752	.3694	
N	1.1370	1.5345	1.4313	1.2286	1.1028	1.4197	.7146	
	1.0368	1.3977	1.2595	1.1194	1.0116	1.3069	.6571	
	A-01	L-05	E-12	A-01	O-01	E-04	A-01	
	.9522	1.0526	1.3192	1.2642	1.0749	.5165		
O	1.1014	1.2558	1.5633	1.5688	1.4191	.9173		
	1.0026	1.1485	1.4299	1.4390	1.3064	.8466		
	E-13	O-01	L-05	D-05	D-05	A-01		
	1.2138	1.2116	1.1320	.6363	.3694			
P	1.4624	1.5040	1.4862	1.0276	.7145			
	1.3402	1.3768	1.3620	.9477	.6571			
	D-05	K-04	E-04	A-01	A-01			
	.6225	.5488	.4027	Assembly Average Power				
R	.9786	.9104	.7635	Assembly Max Fq				
	.8937	.8321	.6952	Maximum 2-D Pin Power				
	A-01	A-01	A-01	Maximum 2-D Pin Power Location				

The maximum assembly power is 1.3192 in assembly O-10.

The maximum Fq factor from 3PINP is 1.5688 in assembly O-11.

The maximum 2-D pin power is 1.4390 in assembly O-11 for pin D-05.

Figure 6
O2C29 Conceptual Core Design
Maximum FΔH as a Function of Cycle Exposure

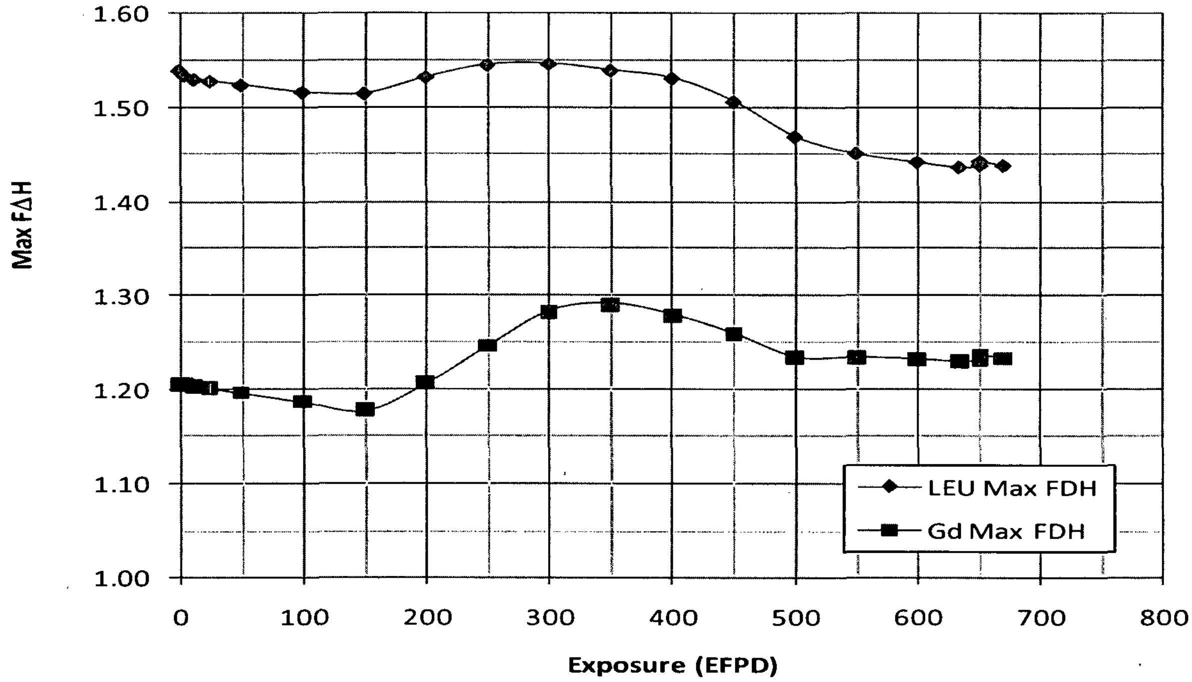

Figure 7
O2C29 Conceptual Core Design
Maximum Fq as a Function of Cycle Exposure

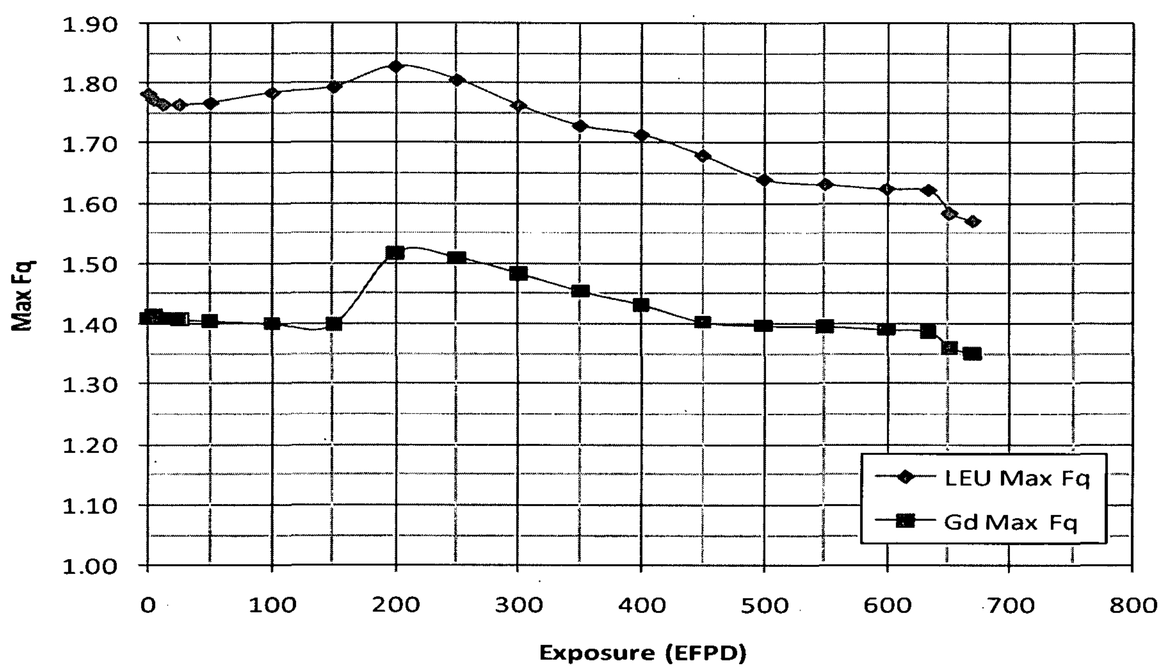

Figure 8
Integrated Pin Power Distribution for Core Location K-12 at 4 EFPD
4.50 w/o U-235 HTP Fuel Assembly with 20 GAD pins (12 pins at 4w/o Gd_2O_3 & 8 pins at 8 w/o Gd_2O_3)

Figure 9
Integrated Pin Power Distribution for Core Location K-12 at 200 EFPD
4.50 w/o U-235 HTP Fuel Assembly with 20 GAD pins (12 pins at 4w/o Gd_2O_3 & 8 pins at 8 w/o Gd_2O_3)

Figure 10
Integrated Pin Power Distribution for Core Location K-12 at 400 EFPD
4.50 w/o U-235 HTP Fuel Assembly with 20 GAD pins (12 pins at 4w/o Gd_2O_3 & 8 pins at 8 w/o Gd_2O_3)

Figure 11
Integrated Pin Power Distribution for Core Location K-12 at 670 EFPD
4.50 w/o U-235 HTP Fuel Assembly with 20 GAD pins (12 pins at 4w/o Gd_2O_3 & 8 pins at 8 w/o Gd_2O_3)

Figure 12
Integrated Pin Power Distribution for Core Location K-14 at 4 EFPD
4.81 w/o U-235 HTP Fuel Assembly with 16 GAD pins (8 pins at 4 w/o Gd_2O_3 & 8 pins at 8 w/o Gd_2O_3)

Figure 13
Integrated Pin Power Distribution for Core Location K-14 at 200 EFPD
4.81 w/o U-235 HTP Fuel Assembly with 16 GAD pins (8 pins at 4 w/o Gd_2O_3 & 8 pins at 8 w/o Gd_2O_3)

Figure 14
Integrated Pin Power Distribution for Core Location K-14 at 400 EFPD
4.81 w/o U-235 HTP Fuel Assembly with 16 GAD pins (8 pins at 4 w/o Gd_2O_3 & 8 pins at 8 w/o Gd_2O_3)

Figure 15
Integrated Pin Power Distribution for Core Location K-14 at 670 EFPD
4.81 w/o U-235 HTP Fuel Assembly with 16 GAD pins (8 pins at 4 w/o Gd_2O_3 & 8 pins at 8 w/o Gd_2O_3)

Q3: As compared to the previously approved methodology in Revision 0 of DPC-NE-1005-PA using the CASMO-4 and SIMULATE-3 MOX codes, what changes have been made to the codes for the methodology presented in Appendix B of DPC-NE-1005-P? Please provide all the changes to the CASMO-4 and SIMULATE-3 codes for the benchmarking comparisons of cores containing gadolinia presented in Appendix B of DPC-NE-1005-P. Please provide the technical basis for these changes.

Q3 RESPONSE:

CASMO-4 and SIMULATE-3 code changes have been made. However, the changes made are minor in nature and are part of the normal evolution of the software to improve accuracy, correct errors and enhance usability. The code changes made to CASMO-4 and SIMULATE-3 since DPC-NE-1005-PA Revision 1 fall into the category of minor changes and are not presented. The code changes made to CASMO-4 and SIMULATE-3 since DPC-NE-1005-PA Revision 0 that were associated with minor PWR method changes were addressed in DPC-NE-1005-PA, Rev. 1 RAI response to question # 3.

Q4: Page B3-5, first paragraph says that the Sequoyah measured incore signals are converted to power using conversion factors derived from cycle-specific core models. For this comparison, were the conversion factors calculated using your own methodology with SIMULATE-3, or did you receive them from Sequoyah? Please describe, in detail, how these conversion factors are calculated. If you calculated the conversion factors, did you compare them to the factors used by Sequoyah?

Q4 RESPONSE:

This question is not applicable to DPC-NE-1006-A because Oconee has a different incore detector system and methodology for processing the signals. The Oconee and TMI incore detector systems are described in Sections 3.1.5 and 3.2.5, respectively. Both Oconee and TMI have similar incore detector systems and analytical schemes for processing and conversion of the raw incore detector signal. The incore signal-to-power factors are derived using cycle specific core models using nuclear physics codes implemented at the time of the measurement. Detailed description of the incore detector signal processing and conversion is described in DPC-NE-1004-A, RAI response to Question 11.

The TMI fuel assembly power distribution benchmark analysis was performed using fuel assembly power distribution data as obtained from TMI.

Q5: Page B3-5, paragraph 3, sentence 4 describes the statistical methods used for determining uncertainties and refers to Section 3 of the report. Section 3 indicates that the data must pass a normality test at the 1% significance level. If a data set fails, then "a conservatively large uncertainty is determined". Did any of the data sets that were analyzed in this section fail the test for normality? If so, what statistical method was used to determine a conservatively large uncertainty? Please provide a reference to the statistical method used.

Q5 RESPONSE:

The statistical methodologies for determining the uncertainty for "normal" and "non-normal" distributions, as determined by the normality test, is outlined in detail in paragraph 3 of Section

3.1.5 of DPC-NE-1006-P. For all statistical methodology applications in the report the tables summarizing the uncertainty results also show the outcome of the normality test and the statistical methodology used to determine the uncertainties, refer to Tables 3-5, 3-12 and 4-2.

Q6: Page B3-5, the equation for Observed Nuclear Reliability factors (ONRFs) is given. Please define how the bias term is calculated. Also, $K_a\sigma_a$ is referred to as the statistical deviation of the comparisons. Please provide a specific definition of this term. Is $K_a\sigma_a$ equivalent to the 95/95 one-sided upper tolerance uncertainty on the bias?

Q6 RESPONSE:

Definition of the bias and $K_a\sigma_a$ terms is provided in Section 3.1.5 of DPC-NE-1006-P.

Q7: Section B4.2 indicates that LEU fuel pin power predictions were compared to measurements from the B&W critical experiments for cores 5, 14, and 20 containing gadolinia. Were there other core configurations in the B&W critical experiments that contained gadolinia? Were there other critical experiments that were considered for benchmarking? Please provide the technical basis for why cores 5, 14, and 20 were chosen and other core configurations were excluded from comparisons. Please provide a discussion of how these core configurations compare to the gadolinia core configurations proposed at MNS and CNS.

Q7 RESPONSE:

The methodology for determining the pin power distribution uncertainties associated with the B&W critical experiments, obtained from DPC-NE-1005-PA, Revision 1, is qualitatively described in Section 4.1 of DPC-NE-1006-P. The B&W critical experiments cover a subset of expected gadolinia core geometries and concentrations expected to be used in future Oconee cores. As a result additional benchmarking of CASMO-4/SIMULATE-3 was warranted. The additional benchmarking is quantitatively described in Section 4.3 (paragraphs 2 – 5). The calculations performed encompass the expected core geometries, gadolinia concentrations and burnup ranges expected to be used in future Oconee cores.

The Babcock & Wilcox (B&W) critical experiments described in Reference 6 were performed to develop experimental data for the purpose of verifying the predictive capability of nuclear models to calculate the behavior of uranium-gadolinia (UO_2+Gd_2O_3) burnable absorbers in PWR fuel. A series of 23 critical experiments were conducted, 17 of which contained gadolinia bearing fuel rods. Power distribution measurements were only performed for 6 of the critical experiments. Of the 6 power distribution measurements performed, only 3 of the cores (cores 5, 14 and 20) contained gadolinia. Each of these gadolinia cores was modeled and the results presented in Section B4 of DPC-NE-1005-PA, Rev. 1. The evaluation and the results from the evaluation of the non-gadolinia cores (cores 1, 12 and 18) were presented in Section 4 of DPC-NE-1005-PA, Revision 0.

The remaining B&W gadolinia critical experiments were performed to determine the reactivity worth of UO_2+Gd_2O_3, AG-In-Cd and B_4C rods. Since power distribution measurements were not available for these cores, they were not modeled. A literature search was also performed to identify other non-proprietary PWR gadolinia critical experiments for use in benchmarking CASMO-4/SIMULATE-3 calculated pin powers. No suitable non-proprietary gadolinia critical experiment data was found.

The evaluation of cores 5, 14, and 20 with CASMO-4 was performed as described in DPC-NE-1005-PA, Revision 1, Section B4.3 and the RAI response to question 7 of the same report to demonstrate that the CASMO-4 nuclear models were capable of accurately predicting the local pin power distribution for core configurations containing both UO_2 (LEU) and gadolinia (GAD) fuel pins, and to generate the data needed to develop a predicted to measured gadolinia pin power uncertainty.

Fuel assemblies with up to 20 GAD pins containing between 2 and 8 w/o Gd_2O_3 are initially planned to control core reactivity and provide peaking control for Oconee core designs with gadolinia. Since the critical benchmarks only covered a subset of expected gadolinia rod geometries and concentrations, additional benchmarking of SIMULATE-3 was warranted. The evaluation of the B&W critical experiments, and the benchmark calculations performed in Reference 4, established that CASMO-4 can accurately model fuel lattices with gadolinia. Since the accuracy of the CASMO-4 analytical models was demonstrated, the next step was to use CASMO-4 to expand the test matrix beyond the gadolinia geometries and concentrations modeled in the critical experiments to model lattice geometries representative of those expected in future core designs.

CASMO-4 was used to generate power distributions that were representative of gadolinia fuel assembly designs and fuel assembly configurations that may occur in-reactor to confirm the acceptability of the pin power reconstruction models in SIMULATE-3. This approach was adopted to qualify the SIMULATE-3 pin power reconstruction model because the critical experiments only provided a limited set of benchmarks, and is the reason why the formulation to determine the SIMULATE-3 GAD pin power uncertainty is different from that of the LEU pin power uncertainty. A matrix of theoretical 2x2 geometry lattice calculations were set up to represent gadolinia concentrations and rod configurations representative of those that may be used in future core designs. The 2x2 case matrix accounted for various combinations of fuel enrichment, burnup, LBP, gadolinia concentration and number of gadolinia pins. The 2x2 fuel lattices modeled contained anywhere from 8 to 20 gadolinia pins ranging from 2 to 8 w/o Gd_2O_3. The 2x2 configurations evaluated are shown in Figure 4-1. The fuel combinations modeled are representative of the gadolinia configurations initially planned for the Oconee core designs. As experience is gained, and cycle design energy requirements change, it is expected that the number and concentration of gadolinia fuel rods in a lattice may change.

The 2x2 SIMULATE-3 to CASMO-4 power distribution comparisons were used to quantify the accuracy of the pin power reconstruction model in SIMULATE-3. The uncertainty calculated in this step was combined with the CASMO-4 uncertainty calculated from comparisons against measured data from the B&W critical experiments to generate a total SIMULATE-3 pin power distribution uncertainty for gadolinia fuel.

Q8: Please provide the formulation for obtaining the uncertainty that is reported for LEU fuel pin power at the bottom of Table B4-3. Does this calculation use the same formula as the gadolinia pin uncertainty that is shown on page B4-4?

Q8 RESPONSE:

The methodology applied to determine the LEU and GAD pin power uncertainties is the same methodology used in DPC-NE-1005-PA, Revision 1. No formulation is provided since the methodology is incorporated by reference.

Q9: Please provide the formulation for the bias term that is used in the calculation of uncertainty for LEU pin power and gadolinia pin power.

Q9 RESPONSE:

The only pin power uncertainty calculated in DPC-NE-1006-P is the gadolinia CASMO-4 to SIMULATE-3 reconstruction uncertainty (refer to Section 4.3, paragraphs 2 - 5). The other pin power uncertainty values are obtained from DPC-NE-1005-PA, Rev. 1.

The formulation for the bias - defined as the mean relative error between SIMULATE-3 and CASMO-4 calculated gadolinia pin power is as follows:

$$Bias = \bar{x} = \frac{\sum_{i}^{n} \frac{(S_i - C_i)}{C_i}}{n}$$

Where: S_i = the i[th] SIMULATE-3 calculated pin power,
C_i = the i[th] CASMO-4 calculated pin power,
n = the sample size

Q10: Page B4-4, first paragraph, why was the measured gadolinia pin power assumed to be [ ]? Please provide the technical bases that were used in choosing this specific number.

Q10 RESPONSE:

The technical basis for the assumed GAD pin power, as described in DPC-NE-1005-PA, Revision 1, RAI response to question #10, remains unchanged for the Oconee application. The gadolinia CASMO-4 predicted to measured pin power uncertainty is obtained from DPC-NE-1005-PA, Revision 1 (page B4-4, as referenced in Section 4.3, paragraph 1 of DPC-NE-1006-P) and therefore this calculation is not repeated in DPC-NE-1006-P.

Q11: On page B4-4, in the last sentence of the last complete paragraph, a best estimate 95% tolerance one sided uncertainty of [ ] is shown. Please provide the formulation for obtaining this value. Please provide additional clarification to this paragraph.

Q11 RESPONSE:

The CASMO-4 predicted to measured GAD pin power best estimate (i.e. statistically large sample size) one-sided 95% tolerance uncertainty was provided in DPC-NE-1005-PA, Revision 1 (page B4-4) to demonstrate the conservatism in calculated GAD pin power one-sided 95% tolerance uncertainty from the actual sample size. Since the calculated GAD pin power one-sided 95% tolerance uncertainty was incorporated in DPC-NE-1006-P by reference (DPC-NE-1005-PA, Revision 1, page B4-4) the best estimate gadolinia CASMO-4 predicted to measured uncertainty is not mentioned in DPC-NE-1006-P.

Q12: In Table B4-4, was a test for normality performed on the data that is reported in this table? If so, please provide the results of the normality test. Was a non parametric uncertainty considered for this data? Please provide the quantitative basis for treating this data set as a normal distribution.

Q12 RESPONSE:

Table B4-4 of DPC-NE-1005-PA, Revision 1 summarizes the gadolinia CASMO-4 predicted to measured uncertainty. The associated normality test evaluation is documented in DPC-NE-1005-PA, Revision 1 response to RAI question #12. The gadolinia CASMO-4 predicted to measured uncertainty documented in DPC-NE-1006-P (Section 4.3) is obtained by reference from DPC-NE-1005-PA, Revision 1 (Table B4-4).

Q13: Was an uncertainty analysis performed for the comparison of gadolinia pin powers calculated with SIMULATE-3 and the measured pin powers from the B&W critical experiments? If available, please provide the results of this comparison. Also, please provide the qualitative and quantitative technical basis for why the CASMO-4 predicted gadolinia pin powers are used for the uncertainty analysis, rather than those from SIMULATE-3.

Q13 RESPONSE:

The methodology for the determination of the gadolinia pin power uncertainty was obtained from DPC-NE-1005-PA, Revision 1 and is referenced in Section 4.3. The gadolinia fuel pin power uncertainty is determined by statistically combining the SIMULATE-3 gadolinia fuel pin power reconstruction uncertainty with the CASMO-4 uncertainty determined from the CASMO-4 evaluation of the B&W critical experiments. The B&W critical experiments CASMO-4 predicted to measured gadolinia pin power uncertainty is obtained from DPC-NE-1005-PA, Revision 1. The SIMULATE-3 gadolinia pin power reconstruction uncertainty is re-calculated due to the different fuel lattice used for the Oconee cores. The methodology for performing the latter calculation is consistent with the methodology in DPC-NE-1005-PA, Revision 1.

Q14: For the data presented in Table B4-5, please clarify if both the CASMO-4 and SIMULATE-3 predictions of pin powers are normalized to give an assembly average power of 1.0.

Q14 RESPONSE:

The corresponding table in DPC-NE-1006-P is Table 4-1. The CASMO-4 and SIMULATE-3 predicted pin powers were normalized to an average fuel assembly power of 1.0 prior to calculating the statistical data presented in Table 4-1.

Q15: In Table B4-6, what does the value of [ ] represent? Please clarify if this is the number of simulated gadolinia fuel pins. The data in Table B4-5 suggests that there were 236 gadolinia fuel pins modeled. If some data were not considered in the SIMULATE-3 to CASMO-4 uncertainty analysis, then please provide justification for not considering these data.

Q14 RESPONSE:

The corresponding tables in DPC-NE-1006-P are Tables 4-1 and 4-2. The heading in column 2 of Table 4-1 refers to the total number of gadolinia fuel pins per fuel assembly. The CASMO-4 to SIMULATE-3 pin power distribution uncertainty is determined using the fuel pins located in the upper-left quadrant of the lower-right fuel assembly of the 2x2 colorset (as shown graphically just above the key in Figure 4-1). The variable "n" (sample size) is the total number of gadolinia pins in this "quadrant" multiplied by 3 (number of burnup statepoints) over all the 2x2 colorset cases. All gadolinia pin power data in the quadrant for all the colorset cases were considered in the statistical analysis.

Q16: The standard deviations in Table B4-5 and the standard deviation and non parametric uncertainty in Table B4-6 are given in terms of percentage. Please provide the formulation that is used to determine these values. Are the standard deviations and uncertainty divided by a mean value of gadolinia pin power? What value is used? Please provide the technical basis for using the value for mean gadolinia pin power.

Q16 RESPONSE:

The same methodology as described in DPC-NE-1005-PA, Revision 1 was used and is repeated here for completeness. The corresponding tables in DPC-NE-1006-P are Tables 4-1 and 4-2. The formulation for the standard deviation is the normal sample population standard deviation equation – see details below. The formulation for the uncertainty (i.e. the SIMULATE-3 to CASMO-4 gadolinia pin power reconstruction uncertainty) is provided below Table 4-2, and is repeated below. Relative errors are used in the determination of the bias, standard deviation and the uncertainty, as specified in the 5th paragraph of Section 4.3, and therefore there is no need to divide these terms by the mean value of the gadolinia pin powers. The bias and standard deviation are converted to percentage by multiplying by 100.

The formulation for the sample standard deviation is as follows:

$$\sigma = \sqrt{\frac{\sum_{i=1}^{n}(\bar{x}-x_i)^2}{n-1}}$$

Where: $\bar{x}$ = the mean relative error between SIMULATE-3 and CASMO-4 calculated pin powers or defined as bias (refer to response to RAI Question 9 for formulation),
x_i = the i[th] relative error between SIMULATE-3 and CASMO-4 calculated pin powers,
n = the sample size

Since the D' Test determined the sample distribution as "normal" the formulation for the SIMULATE-3 to CASMO-4 gadolinia pin power reconstruction uncertainty is as follows:

$$Uncertainty = -Bias_s + K_s \sigma_s$$

Where: $Bias_s$ = $\bar{x}$ = the mean relative error between SIMULATE-3 and CASMO-4 calculated pin power
K_s = the 95/95 one-sided upper tolerance factor based on the sample size (obtained from Ref. 15),
σ_s = the standard deviation of the relative error between SIMULATE-3 and CASMO-4 calculated pin powers.

NOTE: Subscript "s" denotes that these parameters are associated with SIMULATE-3 and CASMO-4 calculated pin powers.

Q17: On page B4-6, in the gadolinia pin uncertainty formula, please provide a clarification of how the bias term is determined. Is the bias taken from the results of the comparison of CASMO-4 predictions to measured data from the B&W critical experiments, as shown in Table B4-4?

Q17 RESPONSE:

Qualitative details of how the gadolinia pin power distribution bias (i.e. $bias_{PG}$) is calculated are described in Section 4.3 (last paragraph). Formulation and calculation of the gadolinia pin power bias (i.e. $bias_{PG} = bias_c + bias_s$) is shown in Table 4-3. The gadolinia pin power bias is the summation of the CASMO-4 predicted to measured bias (i.e. $bias_c$) from the comparison of CASMO-4 predicted pin powers against measured pin powers from the B&W critical experiments (described in the 1st paragraph of Section 4.3) and the bias term (i.e. $bias_s$) associated with the CASMO-4 to SIMULATE-3 pin power reconstruction uncertainty (described in the 5th paragraph of Section 4.3 and shown in Table 4-2).

Q18: For the values that appear in Table B5-1, please provide specific references to the Tables from earlier sections of this report in which these values appear. For the gadolinia fuel pin uncertainty ($K_p\sigma_p$), please provide a formulation for how this term is calculated.

Q18 RESPONSE:

Specific references for each value (biases and statistical uncertainties) appearing in Table 5-1 and Table 5-2 are listed in Sections 5.2 and 5.3, respectively.

Formulation and calculations of the gadolinia fuel pin uncertainty ($K_{pG}\sigma_{pG}$) and bias ($bias_{PG}$) are provided in Table 4-3.

Q19: Please provide clarification of, and the technical basis for, how the pin biases and pin uncertainties are applied to each of the peaking factors FΔH, Fq, and Fz.

Q19 RESPONSE:

The pin power distribution peaking factors F□H, Fq and Fz 95/95 statistically combined uncertainties (SCUs) developed in Sections 5.2 and 5.3 for all LEU cores and LEU/gadolinia cores, respectively, are composed of biases and statistical uncertainty terms associated with fuel assembly and pin power predicted-to-measurement differences. The power distribution SCUs for the all LEU core and for the LEU/gadolinia core are shown in Tables 5-1 and 5-2, respectively. The predicted pin power distribution is augmented by the applicable power distribution SCU prior to comparison against thermal design limits. A power distribution SCU that is greater than the value specified in Table 5-1 or Tables 5-2 may be used for additional conservatism. For the LEU/gadolinia core the power distribution SCU will be applied to the appropriate fuel pin type as specified in Table 5-2, or a single factor that bounds both the LEU and gadolinia SCU may be applied to all fuel pin types. The application of the power distribution SCUs to the predicted power distribution provides a 95% confidence level that 95% of predicted powers will be greater than measured powers for the parameter of interest.

The application of the power distribution SCUs and other uncertainties in reload design analyses, is described in the methodology reports NFS-1001-A, "Oconee Nuclear Station Reload Design Methodology" and DPC-NE-1002-A, "Oconee Nuclear Station Reload Design Methodology II".

RAI #2:

Tables 3-5, 3-12, and 4-2 provides the statistics for the radial, axial and maximum power distributions. Choose anyone of the Tables and provide a sample calculation for each of the three parameters. That is, show how the D' Test demonstrated that the data sample is "not normal"; how the bias was determined; how the k-sigma value was obtained, and how the uncertainty factor was determined.

RAI #2 RESPONSE:

Table 3-5 is chosen for the sample calculation. The methodology described below is from Section 3.15 of DPC-NE-1006-P. Three types of fuel assembly power peaking factors are calculated which characterize important radial and axial properties of the measured power distributions. Assembly FΔH or assembly radial power is simply the average relative power in each fuel assembly. Assembly Fq or assembly maximum power is the largest relative power in each assembly. Assembly Fz or assembly axial power is the assembly Fq normalized to the assembly radial power (i.e., Fz = Fq / FΔH) for each assembly.

SIMULATE-3 is used to model reactor conditions at which power distribution measurements were recorded during operation of the fuel cycles. Comparison of measured and predicted peaking factors define the relative error in the predicted value for each fuel assembly in each power distribution measurement. The relative error (or deviation) is defined as predicted minus measured divided by the measured assembly power expressed in percent. The uncertainty analysis is performed by comparing the calculated power to the measured power for the power distribution measurements excluding core locations with a normalized measured power less than or equal to 1.0, which is consistent with previous Duke approved methodologies.

One-sided upper tolerance limit uncertainties are developed to ensure with a 95% confidence level that 95% of local power predictions are equal to or larger than the corresponding measured values. The D′ Test (Reference 16), performed at a 1% level of significance (consistent with References 2 and 14), is used to test the normality of each data set.

If the data set is normally distributed per the D′ Test, then the Observed Nuclear Reliability Factors (ONRFs) for $F_{\Delta h}$, F_q, and F_z peaking factors are calculated using the following expressions:

$$ONRF = 1 - Bias + K_a \sigma_a \qquad \text{(Equation 20.1)}$$

Where: $$Bias = \frac{\sum_i^n \frac{(P_i - M_i)}{M_i}}{n} \qquad \text{(Equation 20.2)}$$

P_i is the i[th] predicted or calculated value,

M_i is the i[th] measured value,

n is the sample size,

K_a is the 95/95 one-sided upper tolerance factor based on the sample size (obtained from Ref. 15),

σ_a is the standard deviation of the relative error between predicted and measured data.

The bias term is defined as the mean relative error in the calculated peaking factor. The $K_a \sigma_a$ term represents the statistical uncertainty in the comparison between the measured and predicted data.

If the data set is not normally distributed per the D′ Test, then the ONRFs for the $F_{\Delta h}$, F_q, and F_z peaking factors are calculated using the following "non-parametric" statistical method as follows:

$$ONRF = 1 - E_{mth} \qquad \text{(Equation 20.3)}$$

Where E_{mth} is the m[th] smallest relative error (negative errors indicate that the measured power is greater than the predicted power) for a sample size of n such that there is a 95% confidence level that at least 95% of the population has a relative error greater than this value. The E_{mth} term implicitly includes the bias, thus the statistical uncertainty, $K_a \sigma_a$, can be determined using the following equation:

$$K_a \sigma_a = \text{Bias} - E_{mth} \qquad \text{(Equation 20.4)}$$

The following are the sample results of the Oconee fuel assembly peaking factor ONRF analysis (Ref. Table 3-5). The results from the D' Test indicated that the data sets were not normally distributed (refer to Table 3) and thus the non-parametric statistical method, as described above, was used to determine the Oconee peaking factor ONRFs.

Table 3
Oconee Fuel Assembly Peaking Factor ONRF Statistical Results

RAI #3:

Mixed cores.--- Please provide technical basis as to why the CASMO-4/SIMULATE-3 code suite is applicable to mixed cores.

RAI #3 RESPONSE:

Mixed core models used in the evaluation of transition cores containing dissimilar fuel assembly designs is based on the same methodology that is used to setup a nuclear physics models for a reactor cores containing a single fuel assembly design. The CASMO-4/SIMULATE-3 core model is developed for each reload core design in accordance with the methodology described in this report. For mixed cores, this model contains nuclear cross sections and few group constants for each unique combination of fuel assembly design, enrichment, burnable poison loading type (B_4C lumped burnable poison and/or Gd_2O_3 integral burnable poison) and geometry. The nuclear cross sections and few group constants are derived from explicit single assembly CASMO-4 calculations. The CASMO-4 nuclear data is used by SIMILATE-3 for each fuel design type. The SIMULATE-3 core model models appropriate axial regions and the axial nodalization is set to account for the important axial characteristics of the fuel assemblies.

RAI #4:

How will the non-LOCA transient analyses be impacted by the mixed core, particularly the minimum DNBR calculations?

When a reactor core consists of more than one type of fuel assembly, the flow redistributions due to pressure drop differences in the fuel assemblies of different type might introduce a DNBR penalty with respect to the reference core consisting of only one fuel type. Discuss the impact, if any, of the mixed core on various thermal margin calculations for the proposed new core.

RAI #4 Response:

This response addresses UFSAR Chapter 15 non-LOCA transient and accident methodology issues that are related to a mixed core configuration, containing dissimilar fuel assembly designs co-resident in reload core design. The concern is the possibility that the presence of dissimilar fuel assembly designs in the reactor will introduce the need for special modeling. The main issue is the cross flow that will occur between the two fuel assembly types due to design differences. The following discussion is from Section 7.5 of DPC-NE-2015-PA, "Oconee Nuclear Station Mark-B-HTP Fuel Transition Methodology".

With regard to the modeling of the fuel assemblies in the Oconee RETRAN-3D model, there is no need to model mixed core effects. This conclusion is based on the similarity of the B11 fuel design and the HTP fuel design, the fact that the reactor will be operated at the same thermal-hydraulic conditions regardless of the fuel type, and the coarse modeling (three axial nodes represent the entire core) of the fuel assemblies in RETRAN-3D. The detailed modeling of the fuel assembly will be done using the VIPRE-01 models using input (core average power or heat flux, core inlet flow, core exit pressure, core inlet temperature) from RETRAN-3D. The RETRAN-3D input to the detailed VIPRE-01 modeling of HTP fuel will use either existing RETRAN-3D analysis results with a full core of B11 fuel modeled, or new analyses with a full core of HTP fuel modeled.

With regard to the modeling of the mixed core effects in VIPRE-01 during UFSAR Chapter 15 transients and accidents, the following approach is used. For the applicable Oconee VIPRE-01 models the mixed core effect can be explicitly modeled by including the number and location of each fuel assembly type in each VIPRE-01 model. For example, in a VIPRE-01 model that has different fuel assemblies modeled, the core loading pattern for a mixed core can be used to specifically model the spatial relationship of each fuel assembly type. Also, in lumped channels that combine more than one fuel assembly type, the exact number of each fuel assembly type can be combined when calculating the input for each lumped channel. In addition, a flow mal-distribution factor is applied to the inlet flow to each channel to account for the effect of different lower end fitting pressure losses on the inlet flow distribution. These more detailed approaches for addressing mixed core issues will continue to provide conservative DNBR results.